metals

MDPI

Article

Predicting the Quality of Grain Refiners from Electrical Resistance Measurements of Aluminum

Maja Vončina [1,*], Irena Paulin [2], Jožef Medved [1] and Mitja Petrič [1]

[1] Department for Materials and Metallurgy, Faculty of Natural Sciences and Engineering, University of Ljubljana, Aškerčeva 12, 1000 Ljubljana, Slovenia; jozef.medved@ntf.uni-lj.si (J.M.); mitja.petric@ntf.uni-lj.si (M.P.)
[2] Institute of Metals and Technology, Lepi pot 11, 1000 Ljubljana, Slovenia; irena.paulin@imt.si
* Correspondence: maja.voncina@ntf.uni-lj.si

Abstract: The objective of grain refining is to reduce the size of the primary solidified crystal grains in aluminum alloys, thereby eliminating large columnar grains. Excellent grain refining results can be achieved only when the grain refining agent is of excellent quality, i.e., the number of Al_3Ti and TiB_2 particles must be appropriate, the shape and size distribution of the particles must be suitable, the Ti/B ratio must be appropriate, and so on. To evaluate the quality of grain refiners, the electric resistivity was measured on four different grain refiners. The obtained results were supported by differential scanning calorimetry analyses and microstructure analyses. It was found that the quality of a grain refiner can be assessed by measurements of electrical resistance. The lowest electrical resistivity was measured for grain refiner B (Al-3Ti-1B), which had the lowest impurity content and the most suitable number and size distribution of TiB_2 and Al_3Ti particles, as well as the most optimal Ti/B ratio, namely, 3.6. A larger number and size of TiB_2 and Al_3Ti particles, as well as elements such as Fe and Si, and also inclusions, which were also confirmed by DSC analyses, cause a higher electrical resistivity due to a stronger scattering of electrons through the matrix.

Keywords: Al-Ti-B grain-refiners; quality; TiB_2 particles; Al_3Ti particles; electrical resistance measurements

check for updates

Citation: Vončina, M.; Paulin, I.; Medved, J.; Petrič, M. Predicting the Quality of Grain Refiners from Electrical Resistance Measurements of Aluminum. *Metals* **2023**, *13*, 717. https://doi.org/10.3390/met13040717

Academic Editor: Sergey V. Zherebtsov

Received: 1 March 2023
Revised: 30 March 2023
Accepted: 4 April 2023
Published: 6 April 2023

Copyright: © 2023 by the authors. Licensee MDPI, Basel, Switzerland. This article is an open access article distributed under the terms and conditions of the Creative Commons Attribution (CC BY) license (https://creativecommons.org/licenses/by/4.0/).

1. Introduction

The goal of aluminum alloys grain refinement is to reduce the size of the primary solidified crystal grains, thereby eliminating large columnar grains if this cannot be achieved at a reasonable cooling rate. In this way, we can reduce the probability of surface defects during material transformation, improve mechanical properties, and increase castability [1–3].

Al-Ti-B master alloys are commonly utilized to refine aluminum alloys. Research reports [4] indicate that effective grain refinement is possible only when dissolved Ti and TiB_2 particles coexist with a reasonable average radius and a narrow radius distribution. However, conventional grain refinement methods fall short of producing high-quality aluminum alloys because the TiB_2 particles in master alloys have a large radius and a wide radius distribution [4,5]. The heterogeneous nucleation of α-Al nuclei by TiB_2 particles is impeded by the presence of dissolved Ti, which also curbs the growth of α-Al grains through constitutional supercooling. When the concentration of dissolved Ti is low, the α-Al and TiB_2 particles exhibit a large contact angle, which leads to a minor inhibitory effect on α-Al growth, resulting in the refinement of only the columnar grain structure. However, the grain refinement outcome improves, and the transition from columnar to equiaxial is observed when the concentration of dissolved Ti is high. On the other hand, when the concentration of dissolved Ti is above a critical value, the effect on grain refinement remains almost unchanged [5].

Nowadays, Al-5Ti-1B master alloy is the most used grain refiner. It has been reported that the radius of TiB_2 particles, which are generally synthesized by halide salts, gradually

increases, and the radius distribution of TiB_2 particles becomes wider, resulting in limited refining ability. The re-precipitation of TiB_2 particles can improve grain refinement; first, TiB_2 particles with a narrow radius distribution and a small average radius are produced in the Al melt. The resulting melt is then used directly for refining aluminum alloys (referred to as "re-precipitated refinement" in the following) [4].

The morphology of Al_3Ti particles is determined by the ratio of Ti/B in the master alloy and processing conditions, which govern the growth mechanisms. Depending on the specific Al-Ti-B grain refiner, the morphology of Al_3Ti particles may either appear as large blocky particles in the α-Al grain centers while smaller TiB_2 particles are displaced towards the grain boundaries (e.g., Al-5 wt.% Ti-1 wt.% B) or as flaky particles when the Ti/B ratio is decreased (e.g., Al-3 wt.% Ti-1 wt.% B) [5–7]. For the effective nucleation of α-Al, the titanium content in the final melt (with refiner added) must exceed the stoichiometry of TiB_2. A small excess of titanium is sufficient for refining, and higher titanium contents that ensure the survival of Al_3Ti in the melt do not enhance performance. However, it is possible to restore the performance of a refiner that has deteriorated (due to fading or the impact of poisoning solutes) by adding titanium to the melt. The Ti/B weight ratio corresponding to TiB_2 stoichiometry is 2.215, and refining performance significantly improves as this ratio is exceeded but diminishes at higher titanium contents [6,7].

Efforts have been made to comprehend the roles of Ti excess and TiB_2 particles in Al-Ti-B master alloys for grain refinement. Recent research by Fan et al. showed that the high efficiency of TiB_2 particles comes from the formation of an atomic monolayer of a two-dimensional Al_3Ti compound (2DC) on the (0001) TiB_2 surface [8,9]. The formation of Al_3Ti 2DC occurs at the liquid–Al/TiB_2 interface in concentrated Al-Ti solutions and dissolves in diluted Al-Ti solutions. The dissolution kinetics of Al_3Ti 2DC is relatively slow, leading to the high potency of TiB_2 particles with Al_3Ti 2DC in Al melts for an extended period. Based on these findings, it is considered that Ti excess is unnecessary for grain refinement once Al_3Ti 2DC forms on the TiB_2 surface. Hence, using master alloys containing high-efficiency TiB_2 particles with Al_3Ti 2DC but no Ti excess for refining Al should lead to good refining efficiency and improved electrical conductivity of aluminum [8].

The effectiveness of Al-Ti-B master alloys in grain refinement can be significantly diminished by the presence of certain alloying or impurity elements in Al alloys, including Zr, Cr, and Li, as well as high Si content [9–13]. This phenomenon is commonly referred to as "poisoning" in the literature [9]. Research has shown that even small amounts (a few hundred ppm) of Zr in the Al melt can render commercial Al-5Ti-1B grain refiners ineffective, resulting in a coarse and completely columnar grain structure upon solidification. Notably, there is no segregation of Fe or Si at the basal surface of TiB_2, although Fe does segregate at the prismatic surface {1 0 -1 0} of TiB_2. Neither Fe nor Si, as impurity elements, appear to play a role in the Zr poisoning of TiB_2 particles in the Zr-containing Al melt [9]. It was shown that heterogeneous nucleation can be effectively influenced, i.e., either enhanced or hindered, by the chemical segregation of selected alloy/impurity elements at the liquid–substrate interface [8].

Pure aluminum is known for its excellent electrical conductivity due to its low electrical resistivity. However, the presence of impurities can significantly affect its electrical properties. The purity of aluminum is the most important factor affecting its electrical resistivity; the higher the impurity content, the higher the electrical resistivity [14]. The impact of silicon on the electrical resistivity of aluminum is relatively small when its concentration is up to 0.006 wt.%, and the Fe/Si ratio is between 0.8 and 3.8. However, increasing the silicon content to 0.15–0.16 wt.% drastically enhances this effect [14]. Other elements, such as chromium, tungsten, manganese, and titanium, have a more significant impact on increasing the electrical resistivity of aluminum. For aluminum intended for the electrical industry, the total concentration of these four elements should not exceed 0.015 wt.% due to this effect. When the silicon content is between 0.12 wt.% and 0.16 wt.%, the total concentration of these four elements must not exceed 0.01 wt.% to meet the industry's requirements [15]. Although aluminum is effectively refined by Al-Ti-B master alloys, the

Ti excess is inevitably introduced into the Al matrix after refinement, which reduces the electrical conductivity [14,16].

Regarding all these facts, by measuring the electrical resistivity, the quality of the grain refiner can be assessed, since it depends strongly on the scattering of electrons. Scattering occurs when electrons do not travel through the crystal lattice without interference [15]. Electron scattering results from thermal vibrations of the lattice that disturb its periodicity, from voids, and from the presence of impurity atoms [15]. In addition, an increase in temperature can cause the thermal oscillation of the network, leading to a separation of atoms in the network and a reduction in the overlap of valence orbitals. As a result, the electrical resistivity increases [15]. Alloys typically exhibit higher electrical resistivity than pure metals [17,18], as the proportion of impurity atoms in the alloy increases. However, if the impurity atoms form phases in the matrix that are rich in the primary element, the resistivity decreases due to reduced electron scattering [15,19–22].

The present work was undertaken to predict the best potential Al-Ti-B grain refiner as a grain refiner for Al alloys. The objective of the present investigation was to evaluate the adequacy of electrical resistivity measurements to assess the most quality grain refiners Al-Ti-B from four different manufacturers, while Al-5Ti-1B and Al-3Ti-1B were studied.

2. Materials and Methods

The composition of the investigated grain refiners and their designations, determined with the inductively coupled plasma optical emission spectrometer ICP-OES (Agilent 720, Santa Clara, CA, USA), are listed in Table 1. These grain refiners were chosen as they are most often used in grain refining of cast and wrought aluminum alloys. Scheil simulation using Thermo-Calc 2022b software 2020a (accessed on 10 February 2023) with a TCAL6 database (Thermo-Calc Software AB, Stockholm, Sweden) was performed for the grain refiners to predict phases formed and relevant mole fractions of all solid phases during solidification. The number of equilibrium phases at room temperature was also calculated.

Table 1. Chemical composition and designations of investigated grain refiners.

Designation	Master Alloy	Prescribed Addition by Manufacturer, g/kg Al	Chemical Element, wt.%						Ti/B Ratio
			Si	Cr	Fe	B	Ti	Al	
A	Al-3Ti-1B	1.2	0.13	<0.01	0.11	0.82	3.5	rest	4.27
B	Al-3Ti-1B	1.2	0.13	<0.01	0.11	0.86	3.1	rest	3.60
C	Al-5Ti-1B	1.2	0.16	<0.01	0.11	0.89	4.9	rest	5.51
D	Al-5Ti-1B	1.5	0.19	<0.01	0.12	0.92	4.8	rest	5.22

For the electrical resistance measurements, the radius of grain refiner wires was measured at 10 places, from which the average radius was calculated. The length of the grain refiner wires was also measured and included in the calculations of the electrical resistivity measurements. The four-probe direct current technique thoroughly described in [23] was used for measurements of the electrical resistivity of the analyzed wires. The electrical resistivity was measured for 10 min at room temperature. The electrical resistivity ρ was calculated using Equation (1):

$$R = \rho \cdot L/A \quad (1)$$

where L is the length and A is the cross-section of the grain refiner wire. The results are given as the resistivity at room temperature for a given grain refining wire in Ωm.

To evaluate the relevance of the obtained electrical resistivity results, all grain refiners were analyzed by differential scanning calorimetry (DSC) and microstructure analysis. DSC tests (DSC 404 F1 Pegasus instrument, NETZSCH Group, Selb, Germany) on all the grain refiners studied were performed with an empty reference corundum pan as scans in a dynamic argon atmosphere. Samples were heated to 720 °C at 10 K/min and then

equilibrated at this temperature for 10 min before being cooled to room temperature at the same cooling rate of 10 K/min. Melting and solidification characteristic temperatures were determined from the recorded DSC curves. Grain refiners were also prepared using a standard metallographic technique. The grain refiners were examined using JEOL JSM-6500F (SEM, JEOL FESEM JSM 6500F, (JEOL, Tokyo, Japan)) equipped with energy-dispersive spectroscopy (EDS, INCA ENERGY 400, Oxford Instruments, High Wycombe, UK) and electron backscatter diffraction (EBSD, camera HKL Nordlys II with Channel 5 software (Oxford Instruments HKL, Hobro, Denmark)) analysis techniques with INCA feature program to analyze the size, shape, and distribution of Al_3Ti and TiB_2 particles.

Finally, the effect and efficiency of the investigated grain refiners were evaluated on Al99.7 aluminum alloy. The test alloy was preheated to 700 °C. After the melting process was completed, the Al-Ti-B master alloy was added to the melt at 1.2 or 1.5 g/kg, depending on the manufacturer's recommendation listed in Table 1. The melt was then held for 2 min and poured at a temperature range of 680–690 °C using a Croning cup, with a cooling rate of about 7 K/min. The samples for grain size determination were taken from the samples prepared in the Croning cup and analyzed in the middle range. The samples were prepared using a standard metallographic technique and then electropolished with Barker's reagent (4% HBF_4) to visualize the grain boundaries. All samples were examined under polarized light using an Olympus BX61 microscope with a DP70 camera (Olympus Europa SE and Co. KG, Hamburg, Germany) at a magnification of 50×. The mean linear section method according to ASTM E112 was used to measure the grain size.

3. Results and Discussion

The Scheil simulation was performed based on the chemical composition of the grain refiners listed in Table 1. The simulation includes an explanation of all the phases that can occur in the experimental grain refiners. The Scheil results in Figure 1 show large differences in the mass fractions of the expected phases during the solidification of the grain refiners. For grain refiners A and B, the TiB_2 phase is expected to solidify before the Al_3Ti phase (marked blue in the Scheil diagram). For grain refiners C and D, the proportion of the Al_3Ti phase is expected to be higher. The solidification process is the same for all grain refiners; only the number of phases and the solidification temperatures are different. Grain refiners C and D contain the highest amount of Al_3Ti phase in equilibrium (Table 2), as expected due to the higher Ti content in the grain refiner. These Al_3Ti particles do not play a role in the grain refinement of the aluminum alloys in the absence of TiB_2 particles. Grain refiner D also contains the highest proportion of Al_9Fe_2Si (or $Al_{13}Fe_4$, depending on the Fe and Si content in the grain refiner, marked purple and orange in the Scheil diagram), which is due to a higher proportion of impurities, such as Fe and Si.

Table 3 shows the electrical resistivity of the grain refiners studied. Grain refiner B has the lowest electrical resistivity, predicting the lowest content of impurities that lower the electrical resistivity [10,16,19–21]. It is expected that this grain refiner contains flaky Al_3Ti particles that are more evenly distributed, which also corresponds to the analyzed Ti/B ratio that enables conditions for an optimal grain refining effect. For grain refiners C and D (Al-5 wt.% Ti-1 wt.% B), the electrical resistivity increases, and the Ti/B ratio increases, suggesting different shapes of Al_3Ti particles, i.e., blocky-like and flaky-like, as reported by some authors [5–7]. The Ti/B weight ratio corresponding to TiB_2 stoichiometry is 2.215; refining efficiency improves significantly when this ratio is slightly exceeded but decreases at higher titanium contents [6,7], as is the case for grain refiners C and D. Grain refiner D also contains higher amounts of Al_3Ti and Al_9Fe_2Si (Table 2) which also decrease the electrical resistivity.

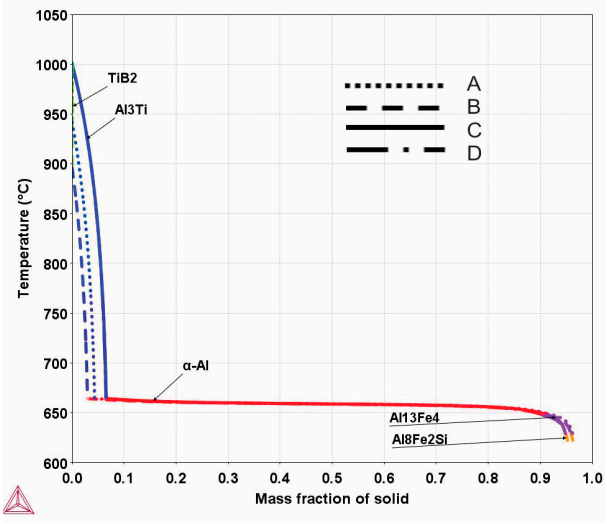

Figure 1. Mass fractions of all solids formed during solidification of investigated grain refiners. The simulation is based on the Scheil model.

Table 2. Mass fraction of equilibrium phases at room temperature in wt.%.

Grain Refiner	TiB_2	Al_3Ti	α-Al	$Al_9Fe_2Si/Al_{13}Fe_4$
A	2.64	4.58	92.37	0.41
B	2.76	3.26	93.57	0.41
C	2.86	7.98	88.75	0.41
D	2.96	7.52	89.08	0.45

Table 3. Specific electrical resistivity of investigated grain refiners.

Designation	L, mm	A, mm^2	R, Ω	P, Ωm
A	800	0.76 ± 0.01	0.000368	3.48×10^{-8}
B	1000	0.76 ± 0.01	0.000443	3.36×10^{-8}
C	1000	0.77 ± 0.01	0.000454	3.48×10^{-8}
D	700	0.24 ± 0.01	0.000341	3.53×10^{-8}

Figure 2 shows the results of the DSC analysis, obtained during cooling. From the DSC curves, the course of the solidification processes of various grain refiners was determined in order to establish a relationship between the phase transformation and the electrical resistivity results. The DSC cooling curves show clear differences between the grain refiners. The solidification temperatures of all characteristic phases (α-Al, Al_3Ti, and $Al_9Fe_2Si/Al_{13}Fe_4$) varied between the studied grain refiners, confirming the different chemical compositions. The variation between the grain refiners was also evident in the solidification enthalpy, which was the lowest for grain refiners C and D. This indicates a higher content of impurities (non-metallic inclusions), which do not melt until 720 °C and are not such effective inoculants. In addition, the impurities can contaminate the TiB_2 particles and reduce the grain refining performance of the grain refiners [24,25].

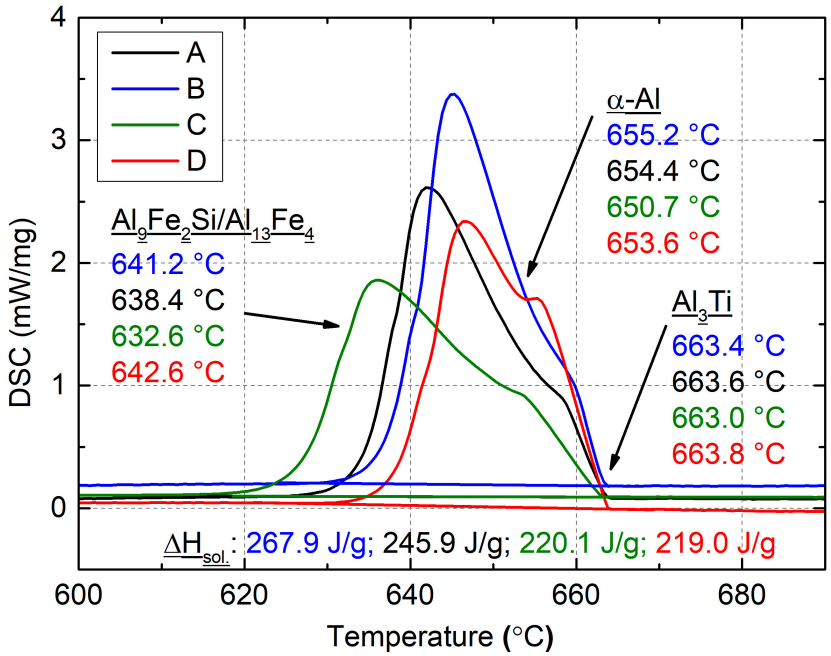

Figure 2. Cooling DSC curves of grain refiners investigated: A (black), B (blue), C (green), and D (red), with the characteristic temperatures, phases, and enthalpies marked.

Figure 3a–h depict typical micrographs of grain refinement in the as-cast state. In Figure 3a,b, which show the Al-3 wt.% Ti-1 wt.% B alloy, large Al_3Ti particles can be seen in a blocky- or flake-like form, which are not uniformly distributed in the matrix, whereas the smaller TiB_2 particles are fragmented in between. Figure 3c,d show the Al-3 wt.%-Ti-1 wt.%-B alloy with quite differently shaped Al_3Ti particles uniformly distributed in a flake-like form. Finally, for grain refiners C and D (Figure 3e–h), which represent the Al-5 wt.% Ti-1 wt.% B alloy, the shape of the Al_3Ti particles changes from blocky to flaky when the Ti/B ratio is reduced. These findings also confirm EDS maps of elemental distributions of elements in the microstructure, presented in Figure 4.

The Al_3Ti and TiB_2 particles were analyzed from multiple micrographs (48) using SEM, focusing on the size distribution, and the results are shown as the number of particles with respect to size (particle surface area) in Figures 5 and 6. Since the size distribution of TiB_2 particles in the grain refiners has a significant effect on the grain refining efficiency, grain refiner B showed the best results, although the others had more TiB_2 particles with very small sizes (from 0.04–0.1 μm^2). However, grain refiners A, C, and D also contained very large particles (0.25–1.0 μm^2). The highest number of TiB_2 particles was found in grain refiner D (41,857 per mm^2), as also predicted by thermo-calc calculations, but due to the uneven size distribution and the highest content of Fe, Si, and other impurities, confirmed by DSC analysis, it is expected not to be the most efficient. Although grain refiner B contains a smaller amount of TiB_2 particles (34,016 per mm^2), its performance should be the best because the size distribution is the most uniform. Additionally, the impurity content is the lowest according to DSC analysis, which also results in the lowest electrical resistivity. The larger particles and the impurities such as Fe, Si, and inclusions cause more electron scattering by the matrix [15].

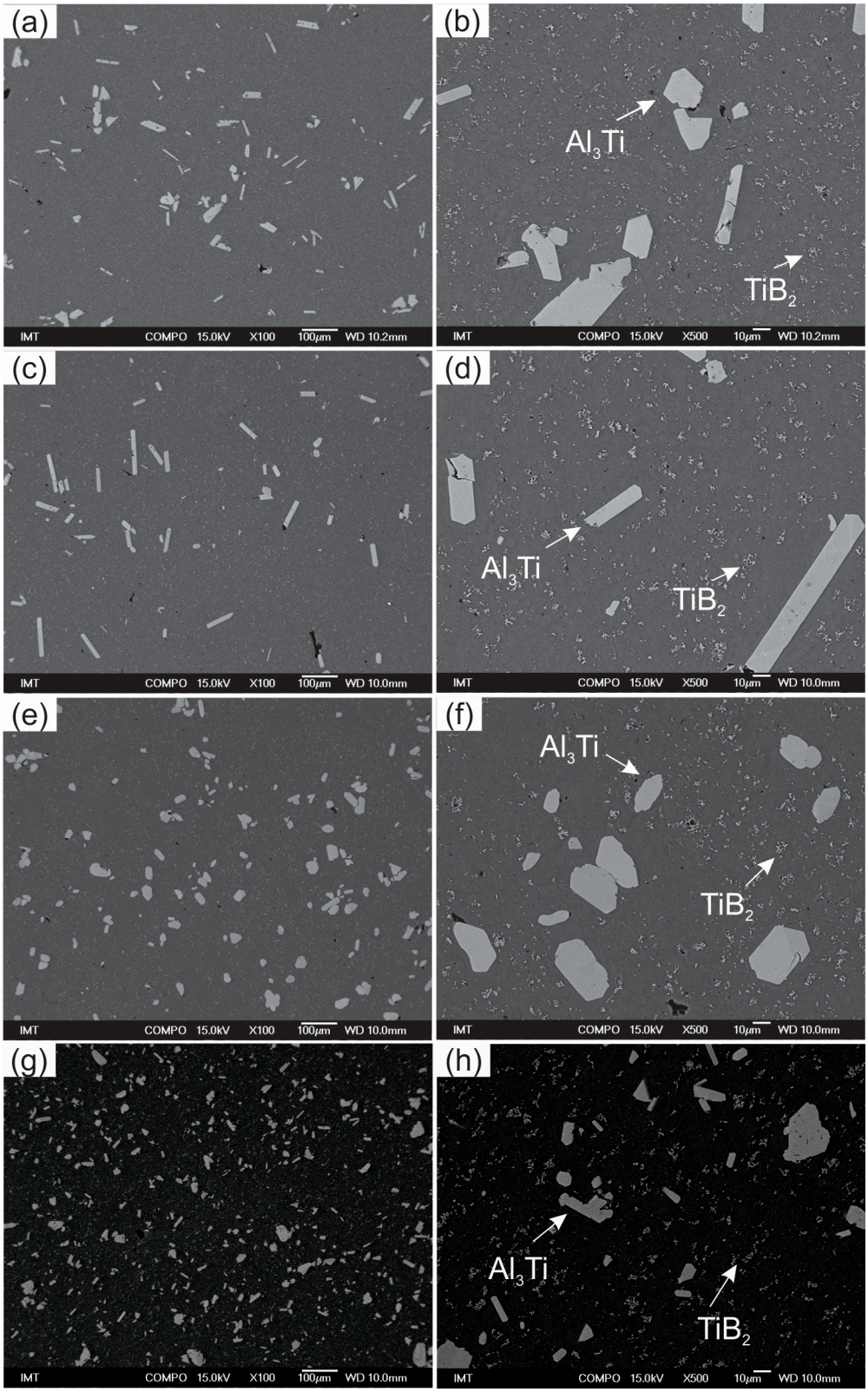

Figure 3. SEM images of investigated grain refiners: (**a**,**b**) A, (**c**,**d**) B, (**e**,**f**) C, and (**g**,**h**) D.

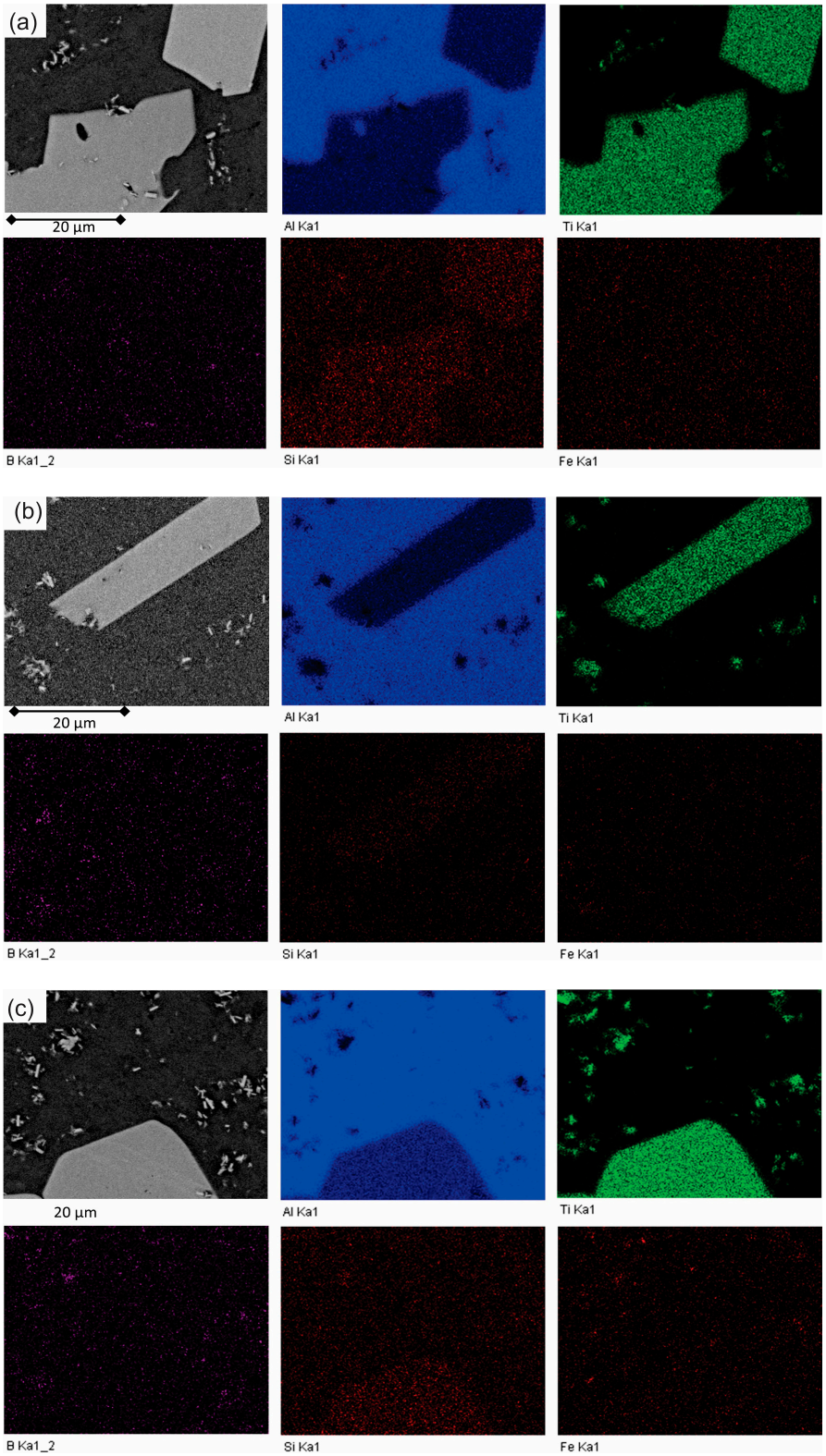

Figure 4. *Cont.*

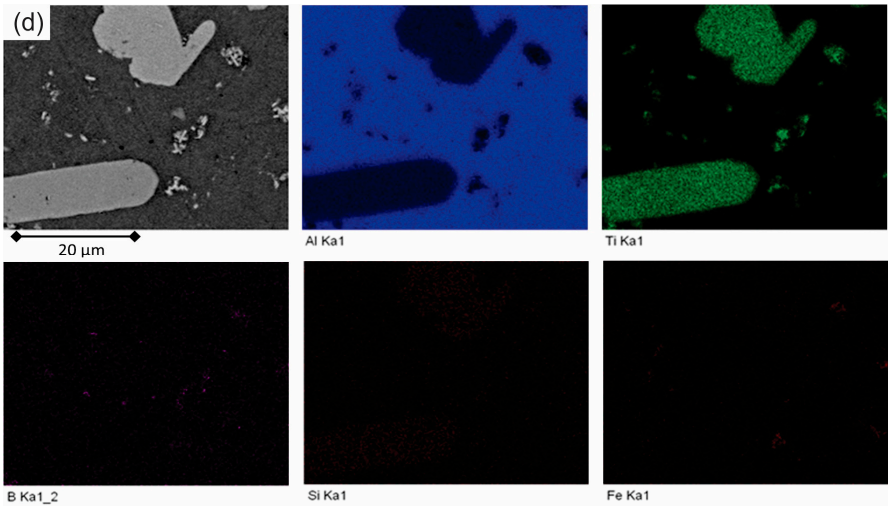

Figure 4. SEM maps of elemental distribution in grain refiner (**a**) A, (**b**) B, (**c**) C, and (**d**) D.

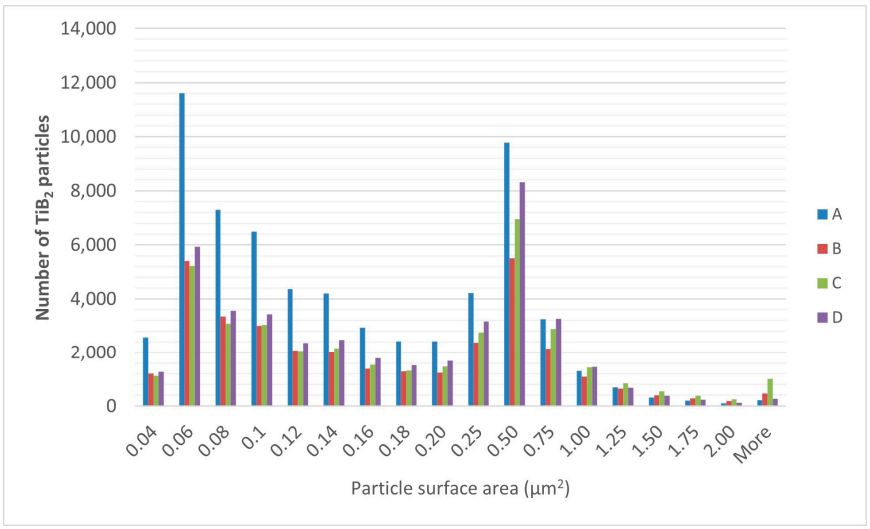

Figure 5. TiB_2 particle size distribution in various grain refiners.

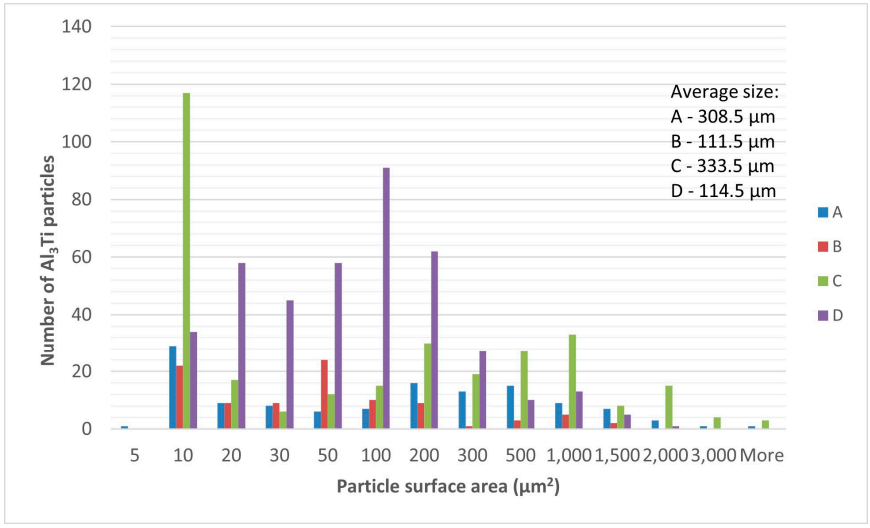

Figure 6. Al_3Ti particle size distribution in various grain refiners.

The different shapes of Al_3Ti particles are shown in Figure 3a–h and can be caused by different growth mechanisms and processing conditions. Both insoluble TiB_2 particles and soluble Al_3Ti particles of appropriate size and shape are required for effective inoculation, with the TiB_2 particles serving as a substrate for Al_3Ti nucleation. Studies show that the number of Al_3Ti particles added to the melt of Al-Ti-B grain refiners has a smaller effect on inoculation than the number of TiB_2 particles [25], suggesting that grain refinement is primarily driven by TiB_2 as a nucleation substrate, with Ti excess having secondary effects on the surface area of TiB_2. However, optimal grain refinement also requires Al_3Ti particles in appropriate concentrations and sizes. In this case, grain refiner B exhibits the most uniform size distribution of Al_3Ti particles, and grain refiners C and D show the largest deviations (Figure 6).

These grain refiners were also tested for their grain refining performance and were found to be fast-acting grain refiners with good efficiency, which was reported in [25]. The first micrograph in Figure 7a shows the typical microstructure of an as-cast Al99.7 aluminum alloy solidified at a cooling rate of ~7 K/min. In this case, the grain size is very large, about 440 µm, as shown in Figure 7a. In contrast, when experimental grain refinement material is added, the grain size is much finer, from 270–370 µm (Figure 7b–e). Improved grain refinement performance was observed with the addition of grain refiner B and, surprisingly, C. This could be due to the particle size distribution, as grain refiners B and C contain only one form of Al_3Ti particles, which are more evenly distributed in the matrix (Figure 3).

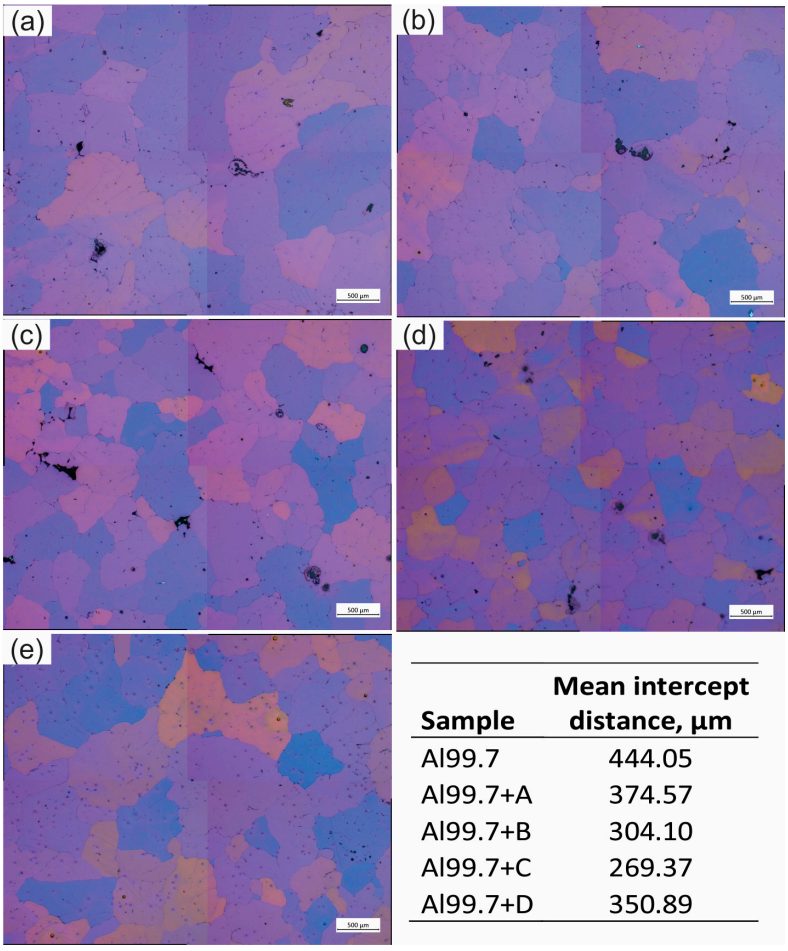

Sample	Mean intercept distance, µm
Al99.7	444.05
Al99.7+A	374.57
Al99.7+B	304.10
Al99.7+C	269.37
Al99.7+D	350.89

Figure 7. Micrographs taken in a polarized light for base aluminum alloy Al99.7 and grain-refined samples using grain refiner A (**b**), B (**c**), C (**d**), and D (**e**). Table in this figure is presenting the mean intercept distance in µm for micrographs presented in (**a**–**e**).

4. Conclusions

The quality of the grain refiner could be assessed by electrical resistivity measurements. The presented results show the lowest electrical resistivity of grain refiner B, which contains the fewest impurities and the most suitable number and size distribution of TiB_2 and Al_3Ti particles, as well as the most suitable Ti/B ratio. A larger number and size of TiB_2 and Al_3Ti particles, as well as soluble elements such as Fe and Si yet inclusions, which are also confirmed by DSC analyses, cause a higher electrical resistivity due to a stronger scattering of electrons by the matrix.

The different shapes of Al_3Ti particles may be due to different growth mechanisms and processing conditions. Both insoluble TiB_2 particles and soluble Al_3Ti particles of appropriate size and shape are required for effective inoculation, with the TiB_2 particles serving as a substrate for Al_3Ti nucleation. Al_3Ti particles of suitable concentration and size are required for optimum grain refinement. The optimum number of TiB_2 particles and the optimum distribution of particle size were found in grain refiner B prepared from Al-3Ti-1B with a Ti/B ratio of 3.6. This grain refiner has an average size of Al_3Ti particles of about 111.5 μm and TiB_2 particles of about 0.30 μm. When adding tested grain refiners into Al99.7 aluminum alloy, the grain size decreases from about 440 μm to 270–370 μm. The best results of grain refinement were observed with the addition of grain refiners B and C, as they contain the most suitable particle size distribution.

Author Contributions: Conceptualization M.V. and M.P.; methodology M.V.; validation, M.V.; formal analysis, M.V., M.P. and I.P.; investigation, M.P. and I.P.; data curation, M.P., I.P. and J.M.; writing—original draft preparation, M.V.; writing—review and editing, M.P., I.P. and J.M.; visualization, M.V. All authors have read and agreed to the published version of the manuscript.

Funding: This research was funded by the Slovenian Research Agency (ARRS) under program grants P2-0344 and P2-0132.

Data Availability Statement: The data presented in this study are available on request from the corresponding author.

Conflicts of Interest: The authors declare no conflict of interest.

References

1. Mackenzie, A.S.; Totten, G.E. (Eds.) *Handbook of Aluminum: Physical Metallurgy and Processes*; CRC Press: New York, NY, USA; Marcel Dekker, Inc.: Basel, Switzerland, 2003; Volume 1.
2. Davis, J.R. *Aluminum and Aluminum Alloys*; ASM International: Novelty, OH, USA, 1993. [CrossRef]
3. Han, L.; Vian, C.; Song, J.; Liu, Z.; Han, Q.; Xu, C.; Shao, L. *Grain Refining of Pure Aluminium, Light Metals*; TMS Aluminium Committee, Springer: Berlin/Heidelberg, Germany, 2012. [CrossRef]
4. Zhang, L.; Jiang, H.; He, J.; Zhao, J. Improved grain refinement in aluminium alloys by re-precipitated TiB_2 particles. *Mater. Lett.* **2022**, *312*, 131657. [CrossRef]
5. Wang, X.; Song, J.; Vian, W.; Ma, H.; Han, G. The Interface of TiB_2 and Al_3Ti in Molten Aluminum. *Metall. Mater. Trans. B* **2016**, *47B*, 3285–3290. [CrossRef]
6. Schumacher, P.; Greer, A.L.; Worth, J.; Evans, P.V.; Kearns, M.A.; Fisher, P.; Green, A.H. New studies of nucleation mechanisms in aluminium alloys: Implications for grain refinement practice. *Mater. Sci. Technol.* **1998**, *14*, 394–404. [CrossRef]
7. Yu, H.; Wang, N.; Guan, R.; Tie, D.; Li, Z.; An, Y.; Zhang, Y. Evolution of secondary phase particles during deformation of Al-5Ti-1B master alloy and their effect on -Al grain refinement. *J. Mater. Sci. Technol.* **2018**, *34*, 2297–2306. [CrossRef]
8. Fan, Z.; Wang, Y.; Zhang, Y.; Qin, T.; Zhou, X.R.; Thompson, G.E.; Pennycook, T.; Hashimoto, T. Grain refining mechanism in the Al/Al–Ti–B system. *Acta Mater.* **2015**, *84*, 292–304. [CrossRef]
9. Wang, Y.; Fang, C.M.; Zhou, L.; Hashimoto, T.; Zhou, X.; Ramasse, Q.M.; Fan, Z. Mechanism for Zr poisoning of Al-Ti-B based grain refiners. *Acta Mater.* **2019**, *164*, 428–439. [CrossRef]
10. Spittle, J.A.; Sadli, S. The influence of zirconium and chromium on the grain-refining efficiency of Al-Ti-B inoculants. *Cast Metals* **1995**, *8*, 247–253. [CrossRef]
11. Qiu, D.; Taylor, J.A.; Zhang, M.-X. Understanding the Co-poisoning effect of Zr and Ti on the grain refinement of cast aluminium alloys. *Metall. Mater. Trans. A* **2010**, *41A*, 3412–3421. [CrossRef]
12. Arjuna Rao, A.; Murty, B.S.; Chakraborty, M. Influence of chromium and impurities on the grain-refining behavior of aluminum. *Metall. Mater. Trans. A* **1996**, *27A*, 791–800. [CrossRef]

13. Arjuna Rao, A.; Murty, B.S.; Chakraborty, M. Role of zirconium and impurities in grain refinement of aluminium with Al-Ti-B. *Mater. Sci. Technol.* **1997**, *13*, 769–777. [CrossRef]
14. Wang, R.L.; He, Z.F.; Tian, S.L. Effect of V, Ti, Cr, Mn on the conductivity of electrical aluminum rod. *Nonferrous Metals Process.* **2009**, *38*, 12–14.
15. Petrič, M.; Mrvar, P.; Medved, J. Changes of Dimensions and Electrical Resistivity during Solidification of Alloys from Al–Si System. Ph.D. Thesis, University of Ljubljana, Ljubljana, Slovenia, 2013.
16. Xu, X.; Feng, Y.; Fan, H.; Wang, Q.; Dong, G.; Li, G.; Zhang, Z.; Liu, Q.; Fan, X.; Ding, H. The grain refinement of 1070 alloy by different Al-Ti-B mater alloys and its influence on the electrical conductivity. *Results Phys.* **2019**, *14*, 102482. [CrossRef]
17. Hatch, J.E.; Association, A.; Metals, A.S. *Aluminum: Properties and Physical Metallurgy*; American Society for Metals: Materials Park, OH, USA, 1984; ISBN 978-0-87170-176-3.
18. McGeer, J.P. *Light Metals: Proceedings of the Technical Sessions*; Metallurgical Society of AIME: Englewood, CO, USA, 1984.
19. Closset, B.; Drew, R.; Gruzleski, J.; Pirie, K. Etude par resistivite electrique de la microstructure des alliages de fonderie Al–Si–Mg traites thermiquement. *Mem. Etudes Sci. Rev. Metall.* **1984**, *81*, 439.
20. Mulazimoglu, M.H.; Drew, R.A.L.; Gruzleski, J.E. The effect of strontium on the electrical resistivity and conductivity of aluminum–silicon alloys. *Metall. Trans. A* **1987**, *18*, 941–947. [CrossRef]
21. Mulazimoglu, M.H.; Drew, R.A.L.; Gruzleski, J.E. The electrical conductivity of cast Al–Si alloys in the range 2 to 12.6 wt pct silicon. *Metall. Trans. A* **1989**, *20A*, 383–389. [CrossRef]
22. Belov, N.A.; Aksenov, A.A.; Eskin, D.G. *Iron in Aluminum Alloys: Impurity and Alloying Elements*; Taylor & Francis: New York, NY, USA, 2002. [CrossRef]
23. Petrič, M.; Kastelic, S.; Mrvar, P. Selection of electrodes for the in situ electrical resistivity measurements of molten aluminium. *J. Min. Metall. Sect. B Metall.* **2013**, *49*, 279–283. [CrossRef]
24. Lee, C.-T.; Chen, S.-W. Quantities of grains of aluminum and those of TiB_2 and Al_3Ti particles added in the grain-refining processes. *Mater. Sci. Eng.* **2002**, *A325*, 242–248. [CrossRef]
25. Vončina, M.; Medved, J.; Jerina, L.; Paulin, I.; Cvahte, P.; Steinacher, M. The impact of Al-Ti-B grain-refiners from different manufacturers on wrought Al-alloy. *Arch. Metall. Mater.* **2019**, *64*, 739–746. [CrossRef]

Disclaimer/Publisher's Note: The statements, opinions and data contained in all publications are solely those of the individual author(s) and contributor(s) and not of MDPI and/or the editor(s). MDPI and/or the editor(s) disclaim responsibility for any injury to people or property resulting from any ideas, methods, instructions or products referred to in the content.